Clemson University
TigerPrints

Publications | Physics and Astronomy

4-2018

A Versatile Carbon Nanotube-Based Scalable Approach for Improving Interfaces in Li-Ion Battery Electrodes

Lakshman K. Ventrapragada
Clemson University

Jingyi Zhu
Clemson University

Stephen E. Creager
Clemson University

Apparao M. Rao
Clemson University, arao@clemson.edu

Ramakrishna Podila
Clemson University, rpodila@clemson.edu

Follow this and additional works at: https://tigerprints.clemson.edu/physastro_pubs

 Part of the Astrophysics and Astronomy Commons

Recommended Citation
Please use the publisher's recommended citation. https://pubs.acs.org/doi/10.1021/acsomega.8b00027

This Article is brought to you for free and open access by the Physics and Astronomy at TigerPrints. It has been accepted for inclusion in Publications by an authorized administrator of TigerPrints. For more information, please contact kokeefe@clemson.edu.

This is an open access article published under an ACS AuthorChoice License, which permits copying and redistribution of the article or any adaptations for non-commercial purposes.

ACS OMEGA

Article

Cite This: ACS Omega 2018, 3, 4502−4508

A Versatile Carbon Nanotube-Based Scalable Approach for Improving Interfaces in Li-Ion Battery Electrodes

Lakshman K. Ventrapragada,[†,‡] Jingyi Zhu,[‡,§] Stephen E. Creager,[†] Apparao M. Rao,*[,‡,§] and Ramakrishna Podila*[,‡,§]

[†]Department of Chemistry and [§]Department of Physics and Astronomy, Clemson University, Clemson, South Carolina 29634, United States

[‡]Clemson Nanomaterials Institute, Clemson, South Carolina 29634, United States

Supporting Information

ABSTRACT: Resistive interfaces within the electrodes limit the energy and power densities of a battery, for example, a Li-ion battery (LIB). Typically, active materials are mixed with conductive additives in organic solvents to form a slurry, which is then coated on current collectors (e.g., bare or carbon-coated Al foils) to reduce the inherent resistance of the active material. Although many approaches using nanomaterials to either replace Al foils or improve conductivity within the active materials have been previously demonstrated, the resistance at the current collector active material interface (CCAMI), a key factor for enhancing the energy and power densities, remains unaddressed. We show that carbon nanotubes (CNTs), either directly grown or spray-coated on Al foils, are highly effective in reducing the CCAMI resistance of traditional LIB cathode materials ($LiFePO_4$ or LFP and $LiNi_{0.33}Co_{0.33}Mn_{0.33}O_2$ or NMC). Moreover, the CNT coatings displace the need for currently used toxic organic solvents (e.g., *N*-methyl-2-pyrrolidone) by providing capillary channels, which improve the wetting of aqueous dispersions containing active materials. The vertically aligned CNT-coated electrodes exhibited energy densities as high as (1) ∼500 W h kg^{-1} at ∼170 W kg^{-1} for LFP and (2) ∼760 W h kg^{-1} at ∼570 W kg^{-1} for NMC. The LIBs with CCAMI-engineered electrodes withstood discharge rates as high as 600 mA g^{-1} for 500 cycles in the case of LFP, where commercial electrodes failed. The CNT-based CCAMI engineering approach is versatile with wide applicability to improve the performance of even textured active materials for both cathodes and anodes.

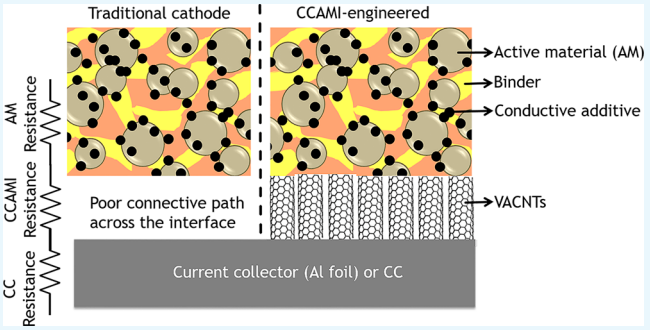

INTRODUCTION

Li-ion batteries (LIBs) are widely used in a variety of devices ranging from portable electronics to power tools and are projected to become the dominant energy storage systems for electric vehicles (EVs)[1] and renewable energy generation technologies (e.g., solar and wind). To this end, the energy and power densities of LIBs must be significantly enhanced with a concomitant improvement in their cycle stability. Prior battery research has focused on identifying new active materials or engineering the microstructure of known active materials[2] for enhancing LIB's energy and power densities. As a result, many methods to synthesize and process cathode and anode active materials with high capacities are now known.[3] Notwithstanding this progress, LIBs still trail due to fundamental limitations arising from the inherent resistive interfaces within the electrode. Most active materials used in LIB electrodes (both anodes and cathodes) are poor electrical conductors and must be mixed with conductive additives for coating on a current collector.[4,5] In a typical LIB cathode (/anode) manufacturing line, an Al (/Cu) current collector is coated (at rates 20 m min^{-1}) with a slurry containing the active material (e.g., $LiFePO_4$ or LFP and $LiNi_{0.33}Co_{0.33}Mn_{0.33}O_2$ or NMC for the cathode and graphite and lithium titanate for the anode), ∼5 wt % conductive carbon (e.g., acetylene black, glucose, and sucrose), and a binder (e.g., polyvinylidene fluoride) in *N*-methyl-2-pyrrolidone (NMP), delivered at rates as high as 150 kg h^{-1}.[6] Thus, different types of interfaces between the grains of the active material, conductive additive, and the current collector are inevitably formed which constitute the total internal resistance (R) of LIBs (Figure 1). Consequently, R results in an undesired voltage drop (or IR drop, where I is the current) and limits the LIB performance at high power. The IR drop increases with the increasing current drawn from the LIB (i.e., higher powers or higher discharge rates) and alters the electrode potential from the equilibrium value leading to a rapid decrease in energy density at higher rates.[7]

The present LIB literature is replete with different procedures for improving the interfaces within the active materials by microstructuring or adding conductive additives such as nanocarbons.[8,9] Notwithstanding this incremental

Received: January 20, 2018
Accepted: April 4, 2018
Published: April 24, 2018

Downloaded via CLEMSON UNIV on September 7, 2018 at 16:26:05 (UTC).
See https://pubs.acs.org/sharingguidelines for options on how to legitimately share published articles.

© 2018 American Chemical Society

DOI: 10.1021/acsomega.8b00027
ACS Omega 2018, 3, 4502−4508

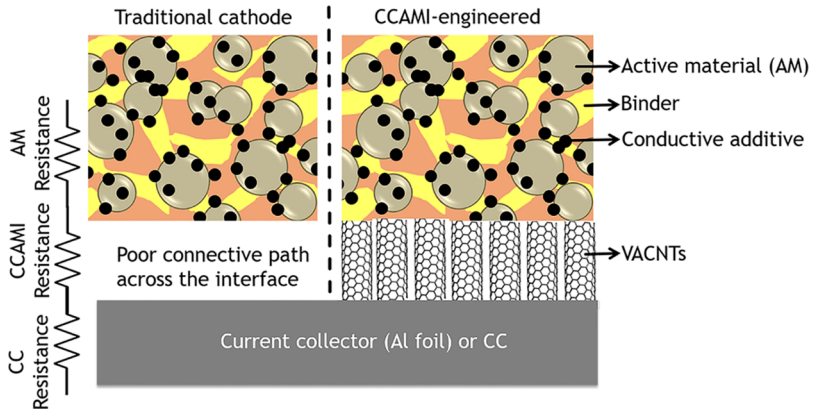

Figure 1. Schematic showing various resistances in LIB cathodes. The overall cathode resistance is the sum of the resistances arising from the (1) active material, binder, and conductive additive coatings, (2) CCAMI, and (3) current collector. As shown on the left, in a traditional cathode, conductive additives decrease the electrical resistance within the active material but do not affect the high CCAMI resistance. On the other hand, as shown on the right, VACNTs directly grown on the Al foil enable better electrical conduction across CCAMI, which dramatically improves the LIB performance.

progress, higher areal capacities, faster charge/discharge rates, or mitigating heating losses (arising from I^2R) and associated hazards in present LIBs remain challenging. Although conventional conductive carbon additives decrease the resistance of interfaces within the cathode/anode active material, they are ineffective in decreasing the current collector active material interface (CCAMI) resistance—a key driving factor for increasing energy and power densities that has largely been ignored in LIBs (Figure 1).

Previously, super-aligned CNTs grown on a Si wafer were drawn into sheets (where the vertical alignment is lost) or coated on a cellulose paper to serve as current collectors for fabricating $LiCoO_2$ cathodes.[10,11] Although such studies replace the traditional Al foil with CNT-based current collectors, they do not address the CCAMI resistance within LIB cathodes. Going beyond existing studies on the use of CNTs in LIBs, we conceptualize and demonstrate a scalable approach for improved CCAMI using vertically aligned CNTs (VACNTs) grown directly on Al foils to enhance LIB electrochemical performance with different cathode-active materials in terms of high rate capability, energy, and power densities. We hypothesize that a thin layer of CNTs, either grown directly or coated on bare Al foils, decreases CCAMI resistance, improves energy densities, and enables stable performance at significantly high powers. CNTs are electrochemically stable,[12,13] and their high electrical conductivity allows for better electron transfer across CCAMI, whereas their high surface-to-volume ratio provides greater ion access. Previously, we demonstrated two roll-to-roll (R2R) processes: (i) a chemical vapor deposition or CVD-based process for growing VACNTs directly on bare kitchen-grade Al foils[14] and (ii) a spray-coating process for coating industrial-grade Al foils with randomly oriented CNTs.[15] Notably, in both of these processes, binders to adhere CNTs to the Al foil are not required. Unlike many methods reported in the literature, our approaches to engineer CCAMI can be readily integrated into LIB manufacturing lines by replacing the traditional current collectors (i.e., Al foils) with CNT-coated Al foils. As delineated below, scalably produced CNT-coated Al foils enhance the performance of different commercially available cathode materials such as LFP and NMC without the need for further modification by reducing the CCAMI resistance by a factor of three. It should be mentioned that the commercially available bulk LFP (manufacturer specified capacity: 145 mA h g^{-1} at C/10) and NMC (manufacturer specified capacity: 145 mA h g^{-1} at C/5) active materials used in this were not textured or coated with carbon. The engineered CCAMI cathodes resulted in as high as >91% enhancements (relative to bare Al foil) in energy density at a power density of 1300 W kg^{-1}. More importantly, CNT-coated cathodes enable LIB performance at very high discharge rates (~600 mA g^{-1}) for up to 500 cycles in the case of LFP, where commercial electrodes were observed to fail. Although textured active materials[16−18] show higher intrinsic capacities relative to commercially available counterparts, they are also limited by CCAMI issues resulting from poor interfacial contact with the current collector. In this regard, the CNT-based CCAMI engineering approach can further improve the performance of even textured LFP and NMC powders with higher intrinsic capacities. In addition to improving the LIB performance, we show that CNT-coated Al foils facilitate active materials to be coated using environmentally benign aqueous slurries instead of expensive and toxic NMP slurries used in the present LIB manufacturing lines. Last, the CNT-based CCAMI engineering approach is versatile and compatible with different types of active materials relevant for both LIB cathodes and anodes (e.g., lithium titanium oxide).

EXPERIMENTAL SECTION

Materials Synthesis. *Growth of VACNTs on Aluminum Foils (Al/VACNTs).* VACNTs were grown on bare Al foils (MTI Corp.) in a two-stage furnace (Thermcraft Inc.) in which the first stage (maintained at 200 °C) served as a preheating zone and the second stage (maintained at 600 °C) served as the reaction zone. A constant flow of ultrahigh purity argon gas (500 SCCM) was maintained throughout the synthesis. Acetylene (30 SCCM) and a ferrocene−xylene mixture (injection rate ≈ 1.5 mL h^{-1}) were introduced into the two-stage furnace in which ~2″ long Al foils were placed at the center of the reaction zone. About 30 μm tall VACNT arrays were obtained on the Al foil in a 30 min long CVD run. Further details on R2R production using this CVD process can be found in ref 14.

Spray-Coated CNTs on the Al Foil (Al/CNT-S). Multiwalled CNTs (Cheap Tubes Inc.) were dispersed in isopropanol (4 mg mL^{-1}) using a tip sonicator and spray-coated onto bare Al

DOI: 10.1021/acsomega.8b00027
ACS Omega 2018, 3, 4502−4508

foils (MTI Corp.) using a paint gun (Iwata 5095 WS400) with 1.3 mm nozzle and 29 psi ambient air pressure. Further details on the R2R spray-coating process can be found in ref 15. The Al foils coated with randomly oriented multiwalled CNTs were used as current collectors for preparing the cathodes which contained LFP, conducting carbon, and the binder.

Electrode Slurry Preparation. The LFP/NMC cathodes were prepared by dispersing $LiFePO_4$ (80 wt %, MTI Corp.) or $LiNi_{0.33}Mn_{0.33}Co_{0.33}O_2$ (80 wt %, electrodes and more), TIMCAL Graphite & Carbon Super P (5 wt %, MTI Corp.), carboxymethylcellulose (CMC, 1 wt %, MTI Corp.), and styrene−butadiene rubber (SBR, 14 wt %, MTI Corp.) in deionized (DI) water (18 MΩ). CMC was first dissolved completely in water at 90 °C, and subsequently, SBR was added to this solution at room temperature. LFP/NMC and carbon Super P were dried, mixed, and added to the above solution under continuous stirring. The resulting slurry was stirred overnight, and an adjustable doctor blade set at 100 μm was used to coat bare Al foils, and commercial carbon-coated Al foils were procured from MTI Corp. (Al/C), Al/VACNTs, and Al/CNT-S foils. Next, the coated Al foils were allowed to dry for 12 h at room temperature and, subsequently, dried at 100 °C for 12 h in a precision compact oven. The LFP and NMC mass loadings in these coatings were ∼3.3 and 2.5 mg cm^{-2}, respectively.

Electrochemical Testing. *Coin Cell Preparation.* Cathodes (dia ≈ 10 mm) were punched, weighed, and soaked in an electrolyte of 1 M lithium hexafluorophosphate ($LiPF_6$) in ethylene carbonate and dimethyl carbonate (w/w = 1:1, Sigma-Aldrich) before assembling them into 2032 type coin cells with a lithium chip (15.6 dia × 0.45 mm thick, MTI Corp.) as the counter electrode. These electrodes were separated by a Celgard 2325 separator (Celgard, LLC) that was presoaked in the electrolyte. The coin cells were assembled inside a glove box where oxygen and moisture contents were below 0.1 ppm.

Galvanostatic Charge/Discharge. Electrochemical characterization was carried out using a Solatron 1470E multichannel potentiostat. LFP cells were initially conditioned by charging and discharging over a potential range of 2.0−4.2 V at a current density of 35 mA g^{-1}. Subsequently, galvanostatic charge/discharge (GCD) studies were performed at varying current densities (50−600 mA g^{-1}) to compare their electrochemical performance. NMC electrodes were tested from 2.5 to 4.3 V at 30 and 150 mA g^{-1}. At the material level, gravimetric energy and power densities were calculated based on the weights of the active materials (LFP or NMC). The energy and power density values at the battery level were estimated as 33% of the values obtained at the material level, following refs 16 and 18.

Electrochemical Impedance Spectroscopy. After conditioning, electrochemical impedance spectroscopy (EIS) was conducted on the cells from 1 MHz to 0.1 Hz, at 0 V versus open-circuit voltage with an ac amplitude of 20 mV.

RESULTS AND DISCUSSION

Figure 2 shows the cross-sectional morphology of Al/VACNTs (panel a) along with those for LFP-coated Al/VACNT, Al/C, and bare Al electrodes (panels (b−d), respectively) as deduced from scanning electron microscopy (SEM, Hitachi S4800). It is evident from Figure 2a that the Al foil is uniformly coated with ∼30 μm tall VACNTs. Thermogravimetric analysis confirmed an equal amount of conductive carbon additives (∼4−5 wt %) in all electrodes[17] (Figure S1).

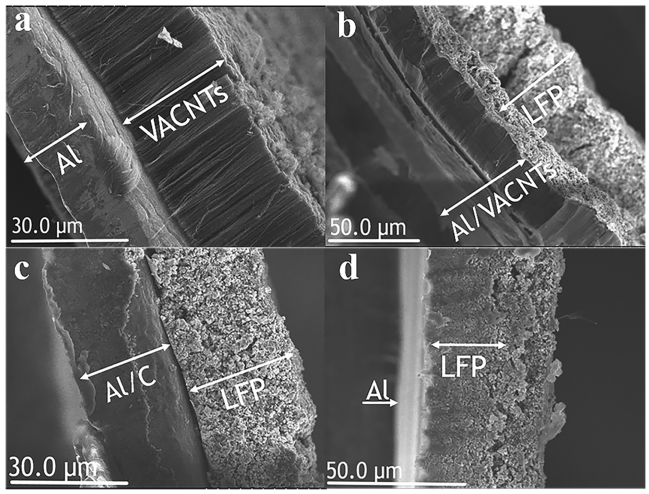

Figure 2. (a) Cross-sectional SEM image of a VACNT-coated Al foil, or Al/VACNT foil. Similar images for LFP coatings on Al/VACNT foil, commercial carbon-coated Al foil, and bare Al foil are shown in panels (b−d), respectively.

As mentioned in the introduction, NMP is currently used in commercial LIB manufacturing for dispersing active materials as its surface tension (41.0 mN m^{-1} at 25 °C) allows good wetting of the Al foil (surface energy: 47.9 mJ m^{-2}). On the other hand, the high surface tension of water (72.8 mN m^{-1} at 25 °C) precludes its use in preparing and coating active material slurries.[19−21] NMP is disadvantageous because of its high cost and toxicity, which warrants the use of expensive solvent recovery systems and stringent protocols for material handling and disposal.[19] The presence of VACNTs on Al provides capillary channels that improve wetting of aqueous dispersions, as evidenced from contact angle measurements shown in Figure S2. The aqueous dispersions exhibited a relatively smaller contact angle (∼60°) on the Al/VACNT-coated foil compared to bare Al foils (∼110°). On the basis of this observation of improved wetting, we replaced NMP with DI water and prepared aqueous slurries to coat both LFP and NMC onto the Al, Al/C, and Al/VACNT foils depicted in Figure 2. We used CMC as the surfactant[22] to increase the suspension stability of LFP or NMC in water, whereas SBR was used as an adhesive to bind the slurries with all of the current collectors.

The GCD responses at two current densities (C/3 and 8C/3 rates; 1 C = 150 mA g^{-1}) for LFP electrodes (viz., Al/VACNTs/LFP, Al/C/LFP, and bare Al/LFP shown in Figure 2b−d, respectively) are shown in Figure 3. The gravimetric capacities for the bare Al/LFP and Al/C/LFP were 90 and 109 mA h g^{-1} at a low current density (50 mA g^{-1}, C/3 rate), respectively (Figure 3a). Consistent with our hypothesis, Al/VACNTs/LFP exhibited a relatively higher gravimetric capacity of ∼145 mA h g^{-1} at the same current density. This implies that >60% enhancement in the gravimetric capacity is possible with CCAMI engineering through VACNTs. Remarkably, as seen in Figure 3b, the Al/VACNTs/LFP collector showed a high areal capacity of 0.55 mA h cm^{-2} at C/3, which is twice the areal capacity of the bare Al current collector (0.26 mA h cm^{-2}). This enhancement in the areal capacity of ∼100% of Al/VACNTs/LFP electrodes (i) brings them closer to the required areal capacity of 1 mA h cm^{-2} for the use of LIBs in EVs[23] and (ii) can be readily accomplished by using Al/VACNT current collectors instead of Al current collectors in the present day LIB

DOI: 10.1021/acsomega.8b00027
ACS Omega 2018, 3, 4502−4508

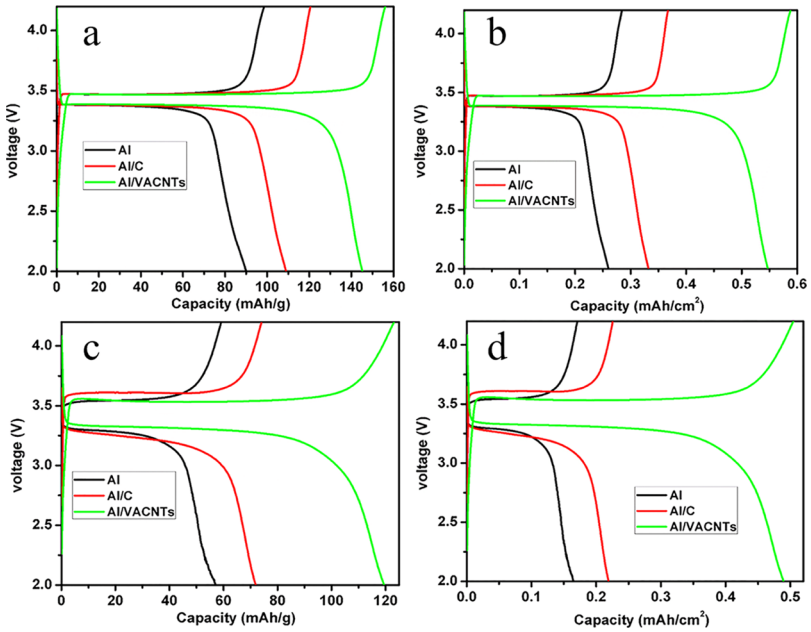

Figure 3. GCD profiles for various current collectors coated with LFP (see text for details). The gravimetric (panels a,c) and areal (panels b,d) capacities at 50 mA g^{-1} (C/3 rate) and 400 mA g^{-1} (8C/3 rate) current densities are shown.

manufacturing lines. At 8C/3 rate, the gravimetric (Figure 3c) and areal (Figure 3d) capacities of Al/VACNTs/LFP exhibited ∼100 and ∼150% enhancements over the corresponding capacities of the bare Al electrode, respectively. Besides investigating the dependence of the gravimetric and areal capacities at low and high current densities, we also examined their dependence on intermediate current densities and summarized them in Figure 4a,b, respectively.

The electrical resistances of the active material (e.g., LFP), current collector (Al), and the CCAMI act in series (cf. Figure 1) and appear as the total internal resistance *R*. Although the addition of conductive carbon (Super P in our case) provides percolating networks within the active material, it does not improve the CCAMI resistance. Previously, it was demonstrated that texturing the Al foil with Al nanoneedles/pillars increased the rate capability and battery performance.[24,25] The underlying mechanism in such methods is to increase the total surface area of the current collector for achieving better contact with the active material. However, such nanostructuring of the Al foil increases its oxidation rate and accelerates the formation of alumina, which could eventually result in the increase of CCAMI resistance leading to battery failure. Here, we present a new scalable process for growing VACNTs directly on Al foils to decrease CCAMI resistance and consequently achieve high rate capability (as shown later in Figure 6a). Traditionally, carbon coatings have also been used on Al foils to reduce the CCAMI resistance and improve the battery performance.[26] Indeed, as shown in Figures 2 and 3, commercial Al/C/LFP electrodes exhibit a moderate improvement over bare Al/LFP. Many commercially available carbon additives such as Super P (added to the active material) contain a mixture of sp^2/sp^3 hybridized carbon.[27] Such carbon additives (Super P in this case) within the active material are known to form highly resistive sp^3 bonds with the carbon coating on the current collector, leading to the failure of LIB cells at high rates.[27] On the other hand, VACNTs not only provide higher surface area but also enable $\pi-\pi$ interactions (as opposed to sp^3 bonds) between sp^2 content of the carbon additives in the active

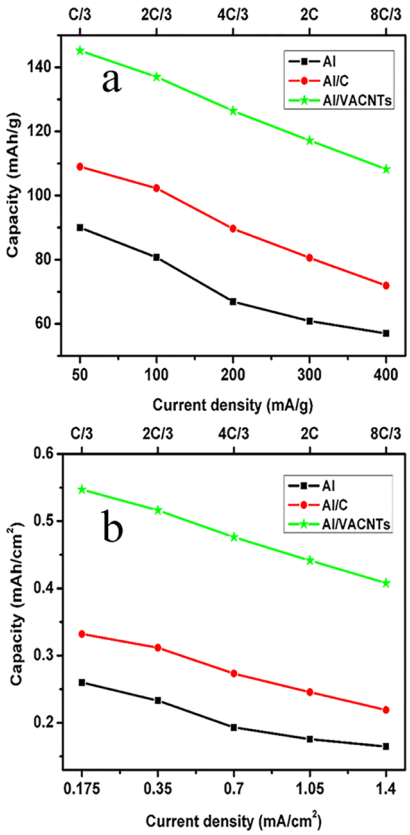

Figure 4. Gravimetric (a) and areal (b) capacities of various LFP electrodes described in Figure 2 at varying current densities (from 50 to 400 mA g^{-1}).

material and CNTs on the current collector to decrease the CCAMI resistance. The changes in equivalent series and charge-transfer resistances (R_s and R_{ct}) resulting from the presence of VACNTs in Al/VACNTs/LFP electrodes were deduced from EIS measurements (Figure 5a). It is well-known

DOI: 10.1021/acsomega.8b00027
ACS Omega 2018, 3, 4502−4508

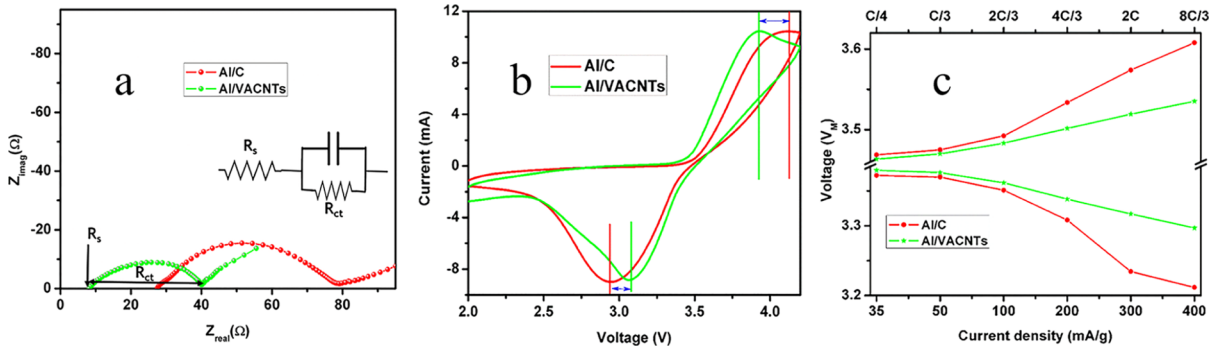

Figure 5. Nyquist plots (a), cyclic voltammograms (10 mV s^{-1}) (b), and mid-point voltages of charge/discharge (c) for LFP electrodes.

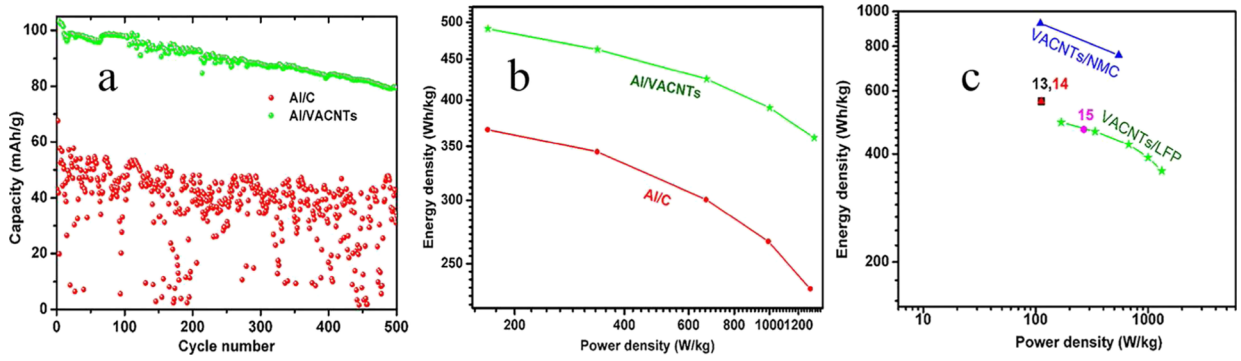

Figure 6. Cyclability (600 mA g^{-1}—500 cycles) (a), energy vs power densities (b), and Ragone plots (c) of current collectors coated with LFP.

that R_s is a series combination of electrolyte and CCAMI resistances.[28] The Nyquist plot for both Al/C/LFP and Al/VACNTs/LFP exhibited a classical single time constant behavior, which was modeled using Randles circuit analysis (see the inset in Figure 5a).[29,30] The R_s values, which is related to the real impedance value in the high-frequency region of the Nyquist plot at Z_{imag} = 0 Ω, were found to be 9.3 and 29.8 Ω for Al/VACNTs/LFP and Al/C/LFP electrodes, respectively. Given that the same electrolyte [1 M $LiPF_6$ in ethylene carbonate and dimethyl carbonate (w/w = 1:1)] was used for all of the cells, the threefold reduction in R_s for Al/VACNTs/LFP is attributed to the presence of VACNTs that significantly reduced the CCAMI. In addition, the characteristic semicircle in the mid- to high-frequency regions, which corresponds to R_{ct}, is relatively lower (∼30 Ω) in the case of Al/VACNTs/LFP electrodes compared to that in Al/C/LFP electrodes (∼50 Ω).[30]

To further characterize our electrodes, we employed cyclic voltammetry to monitor the intercalation/deintercalation of Li^+ at a scan rate of 10 mV s^{-1}. A reduction in the peak potentials during charge/discharge cycles was evident for the Al/VACNTs/LFP electrode, viz., its oxidation peak (∼3.9 V in Figure 5b) is ∼200 mV lower compared to that of the commercial Al/C/LFP electrode (>4.1 V). Thus, the difference between the anodic and cathodic peak voltages is lower for Al/VACNTs/LFP electrodes, which is advantageous in improving the total energy density of the cell within the 2.0−4.2 V window.[17,31] The advantage of VACNTs is also evidenced in the variation of the mid-point voltages (V_M) for both charge and discharge cycles, which is the voltage of the cell when it has discharged 50% of its total energy (Figure 5c). The Al/VACNTs/LFP electrodes showed the least difference (Table S1) in V_M between charge and discharge cycles, which is attributed to lower R due to VACNTs at the CCAMI (Figure 5c). Not surprisingly, Al/C/LFP electrodes exhibited a higher voltage drop, which is attributed to the formation of resistive sp^3 bonds at the interface.[27]

Through our engineered CCAMI with VACNTs, we not only successfully reduced the interfacial resistance but also demonstrated the superior stability of our electrodes at higher current densities up to 4 C or 600 mA g^{-1} (Figure 6a). At this high current density (∼600 mA g^{-1}), the cell can be charged within ∼15 min. The gravimetric capacity of Al/VACNTs/LFP electrodes dropped from 103 to 79 mA h g^{-1} after 500 cycles, which is only a 23% reduction in capacity. On the other hand, the Al/C/LFP electrodes failed to withstand this high current density, which resulted in highly scattered capacity values with an overall deterioration from 67 to ∼0 mA h g^{-1}. Hence, VACNTs on Al improve the stability of the overall electrode by providing a stable contact with the active material during the GCD cycles. Although some groups reported a similar high rate performance of LFP electrodes on bare Al through hierarchical composites or LFP texturing,[16,17] it is worth noting that our process does not require any modifications to commercially used active material powders. Furthermore, the scalable manufacturing processes[32] for VACNT-coated Al foils can be readily integrated into LIB manufacturing lines. Notably, by using Al/VACNTs/LFP electrodes, ∼34 and 54% enhancements in energy densities were realized at power densities of ∼150 and 1300 W kg^{-1}, respectively, as shown in the Ragone plot (Figure 6b,c). The Al/VACNTs/LFP electrode exhibited a drop of 27% in energy density at the highest power of ∼1300 W kg^{-1}, whereas Al/C/LFP showed a 37% decrease (Figure 6b). Notwithstanding the 27% decrease, the energy density of Al/VACNTs/LFP electrodes at the material level is ∼380 W h kg^{-1}, much higher compared to that of ∼230 W h kg^{-1} exhibited by Al/C/LFP, at the highest power density 1300 W kg^{-1}.

DOI: 10.1021/acsomega.8b00027
ACS Omega 2018, 3, 4502−4508

The advantages provided by CNTs were also be realized by spray-coating randomly oriented CNTs on Al foils (Al/CNT-S) using a scalable approach that we had previously developed.[15] We found that Al/CNT-S/LFP electrodes also exhibited a significant enhancement (>58% gravimetric and >78% areal capacities at 400 mA g^{-1}) in the energy and power densities compared to the Al/LFP electrodes (Figure S3). The R2R spray-coating method[15] has a high throughput for coating Al foils (~4 cm^2 s^{-1}) allowing for easy integration into LIB manufacturing lines. Last, to demonstrate the universal nature of CCAMI, we repeated the above measurements using NMC (with equal Ni, Mn, and Co contents) as the active material. The GCD profiles at 30 mA g^{-1} (C/5) and 150 mA g^{-1} (1 C) for different NMC electrodes with and without VACNTs, respectively, are shown in Figure S4. At the material level, the Al/VACNT current collectors coated with NMC showed a very high energy density of 760 W h kg^{-1} at a power density of 570 W kg^{-1}, which corresponds to a 40% increase due to the improved CCAMI in the Al/VACNTs/NMC electrode (Figure 6c).

CONCLUSIONS

We successfully engineered the CCAMI with CNTs on Al current collectors and coated them with aqueous dispersions containing active materials such as LFP and NMC for fabricating LIBs with improved performance, stability, cycle life, high capacity, and energy density. In the case of LFP, a dramatic improvement in the areal (/gravimetric) capacity was observed >100% (/>60%) at low C-rates (<2 C; 1 C = 150 mA g^{-1}) and by >150% (>85%) at high C-rates (>2 C). The CNT-engineered CCAMI resulted in gravimetric energy densities of ~500 and 360 W h kg^{-1} at power densities up to ~170 and ~1300 W kg^{-1} at the material level (corresponding to ~180 and 120 W h kg^{-1} at 70 and 400 W h kg^{-1} at the battery level, respectively) with much higher power capability (increased charge capacity at high discharge rates). Notably, the CNT-modified current collectors with LFP (Al/VACNTs/LFP) withstood rates as high as 4 C for 500 cycles, whereas commercial carbon-coated current collectors coated with LFP (Al/C/LFP) were observed to fail at this rate. For NMC electrodes, the engineered CCAMI with VACNTs exhibited >20% (>35%) improvement in areal (/gravimetric) capacity at 0.2 and 1 C rates (1 C = 145 mA g^{-1}), leading to energy densities as high as ~760 W h kg^{-1} at ~570 W kg^{-1} at the electrode level (~250 W h kg^{-1} at ~190 W kg^{-1} at the battery level).

ASSOCIATED CONTENT

Supporting Information

The Supporting Information is available free of charge on the ACS Publications website at DOI: 10.1021/acsomega.8b00027.

Thermogravimetric analysis, contact angle measurements, mid-point voltage values, additional electrochemical characterization data such as charge/discharge curves, gravimetric and areal capacities, energy versus power density values for Al/CNT-S/LFP electrodes, charge/discharge curves and impedance data for NMC-based electrodes, and additional electron microscopy images (PDF)

AUTHOR INFORMATION

Corresponding Authors

*E-mail: arao@clemson.edu (A.M.R.)
*E-mail: rpodila@clemson.edu (R.P.).

ORCID

Lakshman K. Ventrapragada: 0000-0002-3871-1284
Jingyi Zhu: 0000-0001-7617-0557

Notes

The authors declare no competing financial interest.

ACKNOWLEDGMENTS

This work was financially supported by NSF CMMI SNM grant #1246800. The authors would like to sincerely thank Prof. Joseph Thrasher for his help with TGA analysis, Dr. Ramesh C. Biswal for inputs with the slurry formulation, and Divya T. Vedullapalli for her help with the analysis of GCD data.

REFERENCES

(1) Omar, N.; Daowd, M.; van den Bossche, P.; Hegazy, O.; Smekens, J.; Coosemans, T.; van Mierlo, J. Rechargeable Energy Storage Systems for Plug-in Hybrid Electric Vehicles-Assessment of Electrical Characteristics. *Energies* **2012**, *5*, 2952−2988.

(2) Dimesso, L.; Förster, C.; Jaegermann, W.; Khanderi, J. P.; Tempel, H.; Popp, A.; Engstler, J.; Schneider, J. J.; Sarapulova, A.; Mikhailova, D.; Schmitt, L. A.; Oswald, S.; Ehrenberg, H. Developments in Nanostructured LiMPO4 (M = Fe, Co, Ni, Mn) Composites Based on Three Dimensional Carbon Architecture. *Chem. Soc. Rev.* **2012**, *41*, 5068−5080.

(3) Croguennec, L.; Palacin, M. R. Recent Achievements on Inorganic Electrode Materials for Lithium-Ion Batteries. *J. Am. Chem. Soc.* **2015**, *137*, 3140−3156.

(4) Zhang, W.-J. Structure and Performance of LiFePO4 Cathode Materials: A Review. *J. Power Sources* **2011**, *196*, 2962−2970.

(5) Yuan, L.-X.; Wang, Z.-H.; Zhang, W.-X.; Hu, X.-L.; Chen, J.-T.; Huang, Y.-H.; Goodenough, J. B. Development and Challenges of LiFePO4 Cathode Material for Lithium-Ion Batteries. *Energy Environ. Sci.* **2011**, *4*, 269.

(6) Chung, D.; Elgqvist, E.; Santhanagopalan, S. *Automotive Lithium-Ion Cell Manufacturing: Regional Cost Structures and Supply Chain Considerations*, Denver West Parkway Golden, 2016.

(7) Cao, W. J.; Greenleaf, M.; Li, Y. X.; Adams, D.; Hagen, M.; Doung, T.; Zheng, J. P. The Effect of Lithium Loadings on Anode to the Voltage Drop during Charge and Discharge of Li-Ion Capacitors. *J. Power Sources* **2015**, *280*, 600−605.

(8) Liu, T.; Feng, Y.; Duan, Y.; Cui, S.; Lin, L.; Hu, J.; Guo, H.; Zhuo, Z.; Zheng, J.; Lin, Y.; Yang, W.; Amine, K.; Pan, F. Formation of Mono/bi-Layer Iron Phosphate and Nucleation of LiFePO4 Nano-Crystals from Amorphous 2D Sheets in Charge/discharge Process for Cathode in High-Performance Li-Ion Batteries. *Nano Energy* **2015**, *18*, 187−195.

(9) Lu, J.; Chen, Z.; Ma, Z.; Pan, F.; Curtiss, L. A.; Amine, K. The Role of Nanotechnology in the Development of Battery Materials for Electric Vehicles. *Nat. Nanotechnol.* **2016**, *11*, 1031−1038.

(10) Wang, K.; Luo, S.; Wu, Y.; He, X.; Zhao, F.; Wang, J.; Jiang, K.; Fan, S. Super-Aligned Carbon Nanotube Films as Current Collectors for Lightweight and Flexible Lithium Ion Batteries. *Adv. Funct. Mater.* **2013**, *23*, 846−853.

(11) Hu, L.; Choi, J. W.; Yang, Y.; Jeong, S.; La Mantia, F.; Cui, L.-F.; Cui, Y. Highly Conductive Paper for Energy-Storage Devices. *Proc. Natl. Acad. Sci. U.S.A.* **2009**, *106*, 21490−21494.

(12) Kumar, L. V.; Ntim, S. A.; Sae-Khow, O.; Janardhana, C.; Lakshminarayanan, V.; Mitra, S. Electro-Catalytic Activity of Multiwall Carbon Nanotube-Metal (Pt or Pd) Nanohybrid Materials Synthesized Using Microwave-Induced Reactions and Their Possible Use in Fuel Cells. *Electrochim. Acta* **2012**, *83*, 40−46.

DOI: 10.1021/acsomega.8b00027
ACS Omega 2018, 3, 4502−4508

(13) Kumar, V. L.; Siddhardha, R. S. S.; Kaniyoor, A.; Podila, R.; Molli, M.; Kumar, S. M.; Venkataramaniah, K.; Ramaprabhu, S.; Rao, A. M.; Ramamurthy, S. S. Gold Decorated Graphene by Laser Ablation for Efficient Electrocatalytic Oxidation of Methanol and Ethanol. *Electroanalysis* **2014**, *26*, 1850−1857.
(14) Arcila-Velez, M. R.; Zhu, J.; Childress, A.; Karakaya, M.; Podila, R.; Rao, A. M.; Roberts, M. E. Roll-to-Roll Synthesis of Vertically Aligned Carbon Nanotube Electrodes for Electrical Double Layer Capacitors. *Nano Energy* **2014**, *8*, 9−16.
(15) Karakaya, M.; Zhu, J.; Raghavendra, A. J.; Podila, R.; Parler, S. G.; Kaplan, J. P.; Rao, A. M. Roll-to-Roll Production of Spray Coated N-Doped Carbon Nanotube Electrodes for Supercapacitors. *Appl. Phys. Lett.* **2014**, *105*, 263103.
(16) Wang, B.; Al Abdulla, W.; Wang, D.; Zhao, X. S. A Three-Dimensional Porous LiFePO4 Cathode Material Modified with a Nitrogen-Doped Graphene Aerogel for High-Power Lithium Ion Batteries. *Energy Environ. Sci.* **2015**, *8*, 869−875.
(17) Zhang, K.; Lee, J.-T.; Li, P.; Kang, B.; Kim, J. H.; Yi, G.-R.; Park, J. H. Conformal Coating Strategy Comprising N-Doped Carbon and Conventional Graphene for Achieving Ultrahigh Power and Cyclability of LiFePO4. *Nano Lett.* **2015**, *15*, 6756−6763.
(18) Myung, S.-T.; Maglia, F.; Park, K.-J.; Yoon, C. S.; Lamp, P.; Kim, S.-J.; Sun, Y.-K. Nickel-Rich Layered Cathode Materials for Automotive Lithium-Ion Batteries: Achievements and Perspectives. *ACS Energy Lett.* **2016**, *2*, 196.
(19) Li, J.; Armstrong, B. L.; Kiggans, J.; Daniel, C.; Wood, D. L. Lithium Ion Cell Performance Enhancement Using Aqueous LiFePO4 Cathode Dispersions and Polyethyleneimine Dispersant. *J. Electrochem. Soc.* **2012**, *160*, A201−A206.
(20) Li, J.; Rulison, C.; Kiggans, J.; Daniel, C.; Wood, D. L. Superior Performance of LiFePO4 Aqueous Dispersions via Corona Treatment and Surface Energy Optimization. *J. Electrochem. Soc.* **2012**, *159*, A1152−A1157.
(21) Li, J.; Armstrong, B. L.; Daniel, C.; Kiggans, J.; Wood, D. L. Optimization of Multicomponent Aqueous Suspensions of Lithium Iron Phosphate (LiFePO4) Nanoparticles and Carbon Black for Lithium-Ion Battery Cathodes. *J. Colloid Interface Sci.* **2013**, *405*, 118−124.
(22) Lee, J.-H.; Paik, U.; Hackley, V. A.; Choi, Y.-M. Effect of Carboxymethyl Cellulose on Aqueous Processing of Natural Graphite Negative Electrodes and Their Electrochemical Performance for Lithium Batteries. *J. Electrochem. Soc.* **2005**, *152*, A1763.
(23) Park, O. K.; Cho, Y.; Lee, S.; Yoo, H.-C.; Song, H.-K.; Cho, J. Who Will Drive Electric Vehicles, Olivine or Spinel? *Energy Environ. Sci.* **2011**, *4*, 1621.
(24) Perre, E.; Nyholm, L.; Gustafsson, T.; Taberna, P.-L.; Simon, P.; Edström, K. Direct Electrodeposition of Aluminium Nano-Rods. *Electrochem. Commun.* **2008**, *10*, 1467−1470.
(25) Lecoeur, C.; Tarascon, J.-M.; Guery, C. Al Current Collectors for Li-Ion Batteries Made via an Oxidation Process in Ionic Liquids. *Electrochem. Solid-State Lett.* **2011**, *14*, A6.
(26) Wu, H.-C.; Wu, H.-C.; Lee, E.; Wu, N.-L. High-Temperature Carbon-Coated Aluminum Current Collector for Enhanced Power Performance of LiFePO4 Electrode of Li-Ion Batteries. *Electrochem. Commun.* **2010**, *12*, 488−491.
(27) Swain, P.; Viji, M.; Mocherla, P. S. V.; Sudakar, C. Carbon Coating on the Current Collector and LiFePO4 Nanoparticles—Influence of sp2 and sp3-like Disordered Carbon on the Electrochemical Properties. *J. Power Sources* **2015**, *293*, 613−625.
(28) Wu, Y.; Keil, P.; Schuster, S. F.; Jossen, A. Impact of Temperature and Discharge Rate on the Aging of a LiCoO2/LiNi0.8Co0.15Al0.05O2 Lithium-Ion Pouch Cell. *J. Electrochem. Soc.* **2017**, *164*, A1438−A1445.
(29) Gomez, J.; Nelson, R.; Kalu, E. E.; Weatherspoon, M. H.; Zheng, J. P. Equivalent Circuit Model Parameters of a High-Power Li-Ion Battery: Thermal and State of Charge Effects. *J. Power Sources* **2011**, *196*, 4826−4831.
(30) Waag, W.; Käbitz, S.; Sauer, D. U. Experimental Investigation of the Lithium-Ion Battery Impedance Characteristic at Various Conditions and Aging States and Its Influence on the Application. *Appl. Energy* **2013**, *102*, 885−897.
(31) Liu, M.; Zhao, Y.; Gao, S.; Wang, Y.; Duan, Y.; Han, X.; Dong, Q. Mild Solution Synthesis of Graphene Loaded with LiFePO4-C Nanoplatelets for High Performance Lithium Ion Batteries. *New J. Chem.* **2015**, *39*, 1094−1100.
(32) Arcila-Velez, M. R.; Zhu, J.; Childress, A.; Karakaya, M.; Podila, R.; Rao, A. M.; Roberts, M. E. Roll-to-Roll Synthesis of Vertically Aligned Carbon Nanotube Electrodes for Electrical Double Layer Capacitors. *Nano Energy* **2014**, *8*, 9−16.

DOI: 10.1021/acsomega.8b00027
ACS Omega 2018, 3, 4502−4508